

Equilibrium Molecular Dynamics Simulation Study for Transport Properties of Noble Gases: The Green-Kubo Formula

Song Hi Lee

Department of Chemistry, Kyungsoong University, Busan 608-736, Korea. E-mail: shlee@ks.ac.kr
Received May 30, 2013, Accepted July 9, 2013

This paper presents results for the calculation of transport properties of noble gases (He, Ne, Ar, Kr, and Xe) at 273.15 K and 1.00 atm using equilibrium molecular dynamics (EMD) simulations through a Lennard-Jones (LJ) intermolecular potential. We have utilized the revised Green-Kubo formulas for the stress (SAC) and the heat-flux auto-correlation (HFAC) functions to estimate the viscosities (η) and thermal conductivities (λ) of noble gases. The original Green-Kubo formula was employed for diffusion coefficients (D). The results for transport properties (D, η , and λ) of noble gases at 273.15 and 1.00 atm obtained from our EMD simulations are in a good agreement with the rigorous results of the kinetic theory and the experimental data. The radial distribution functions, mean square displacements, and velocity auto-correlation functions of noble gases are remarkably different from those of liquid argon at 94.4 K and 1.374 g/cm³.

Key Words : Molecular dynamics simulation, Noble gases, Green-Kubo formula, Transport properties

Introduction

Molecular dynamics (MD) simulation is the term used to describe the solution of the classical equations of motion (Newton's equation) for a set of molecules to obtain the dynamic properties of many-particle system.¹ This was first accomplished, for a system of hard spheres, by Alder and Wainwright.^{2,3} In this case, the particle moves at constant velocity between perfectly elastic collisions, and it is possible to solve the dynamic problem without making any approximations, within the limits imposed by machine accuracy.

It was several years before a successful attempt was made to solve the equations of motion for a set of Lennard-Jones (LJ) particles by Rahman.⁴ Here, an approximate, step-by-step procedure is needed, since the forces change continuously as the particles move. Since that time, the properties of the LJ model have been thoroughly investigated.⁵⁻⁷ After this initial groundwork on atomic systems, although many attempts of computer simulations, Monte Carlo (MC) and MD methods, for liquid systems including a diatomic molecular liquid^{8,9} and liquid water^{10,11} were followed, the investigation for gaseous systems by MC and MD has received relatively little attention.

The difference of structural and dynamic properties of gaseous state and liquid state is well known. For example, the radial distribution function of liquid argon at 94.4 K and 1.374 g/cm³ (Fig. 2 in Ref. 4) is completely different from that of gaseous argon at 273.15 K and 1.00 atm, see Figure 1. The difference in the dynamic properties is also remarkable as shown in Figures 2 and 3.

In recent papers,^{12,13} we have examined the Green-Kubo formula for the calculation of the transport properties of liquid argon at 94.4 K and 1.374 g/cm³, using the equilibrium molecular dynamics (EMD) simulation. No problem

is observed in the calculation of the self-diffusion coefficient since the velocity auto-correlation (VAC) function decays to zero fast within 5 ps, where the velocity of each particle is a property of particle. However, for the shear viscosity and thermal conductivity, the stress (SAC) and the heat-flux auto-correlation (HFAC) functions in the Green-Kubo formulas have non-decaying, long-time tails because the stress and the heat flux are system properties, rather than particle properties. Here the system properties indicate properties appeared from a collective behavior of all the molecules in the system, such as temperature, pressure, and heat-flux. By considering the stress and heat-flux of the system as properties of each particle, this problem could be overcome through an N (number of particles)-fold improvement in the statistical accuracy. The results for shear viscosity and thermal conductivity of liquid argon at 94.4 K and 1.374 g/cm³ obtained through the Green-Kubo formula by using a velocity Verlet algorithm for NVT EMD and a fifth-order predict-corrector Gear integration for NpT EMD simulations presented a reasonable agreement with the experimental results.¹³

In this paper, we utilize the revised Green-Kubo for the calculation of the transport properties of noble gases using the EMD simulation. The primary goal of this study is to examine the alternative route for the non-decaying long-time tail of the correlation functions.¹³ In the following section, we present some theoretical aspects. We describe Green-Kubo formula in section II, the molecular models and the technical details of MD simulation in section III, our results in section IV, and the concluding remarks in section V.

Green-Kubo Formula

The Green-Kubo formula for the transport coefficient γ is usually the infinite time integral of an equilibrium correlation function of the form:

$$\gamma = \frac{1}{2} \lim_{t \rightarrow \infty} \frac{d}{dt} \langle [A(t) \cdot A(0)]^2 \rangle, \quad (1)$$

where A is a variable appearing in the perturbation term in the Hamiltonian of the system. Associated with any expression of this kind, there is also the Einstein formula:

$$\gamma = \frac{1}{2} \lim_{t \rightarrow \infty} \frac{d}{dt} \langle [A(t) \cdot A(0)]^2 \rangle, \quad (2)$$

which holds at large t (compared with the correlation time of A).

The common examples are diffusion coefficients from VAC and mean square displacement (MSD):

$$D = \frac{1}{6} \lim_{t \rightarrow \infty} \frac{d}{dt} \langle [\mathbf{r}_i(t) \cdot \mathbf{r}_i(0)]^2 \rangle. \quad (3)$$

and

$$D = \frac{1}{3} \int_0^\infty dt \langle \mathbf{v}_i(0) \cdot \mathbf{v}_i(t) \rangle \quad (4)$$

The original Green-Kubo formula for viscosity is η is given by

$$\eta = \frac{V}{kT} \int_0^\infty dt \langle P_{\alpha\beta}(0) \cdot P_{\alpha\beta}(t) \rangle, \quad (5)$$

where

$$P_{\alpha\beta}(t) = \frac{1}{V} \left[\sum_i m v_{i\alpha}(t) \cdot v_{i\beta}(t) + \sum_i \sum_{j>i} r_{ij\alpha}(t) \cdot f_{ij\beta}(t) \right] \quad (6)$$

and $\alpha\beta = xy, xz, yx, yz, zx, zy$. If the stress is considered as a property of particle, we may write $P_{i\alpha\beta}$ as

$$P_{i\alpha\beta}(t) = \frac{1}{V} \left[m v_{i\alpha}(t) \cdot v_{i\beta}(t) + \sum_{j \neq i} r_{ij\alpha}(t) \cdot f_{ij\beta}(t) \right]. \quad (7)$$

Using this expression, η in Eq. (5) may be rewritten as

$$\eta = \frac{V}{kT} \int_0^\infty dt \sum_i \langle P_{i\alpha\beta}(0) \cdot P_{i\alpha\beta}(t) \rangle. \quad (8)$$

Then the statistical accuracy is improved by N (number of particle) times as large as that of using Eq. (5).

Similarly for thermal conductivity, if the heat flux is considered as a property of particle, we write $\dot{q}_{i\alpha}$ as

$$\dot{q}_{i\alpha}(t) = \frac{1}{V} \left[\varepsilon_i(t) \cdot v_{i\alpha}(t) + \frac{1}{2} \sum_{j \neq i} r_{ij\alpha}(t) \cdot [\mathbf{v}_i(t) \cdot \mathbf{f}_{ij}(t)] \right], \quad (9)$$

where the energy of molecule i is given by

$$\varepsilon_i(t) = \frac{p_i(t)^2}{2m_i} + \frac{1}{2} \sum_{j \neq i} \phi[r_{ij}(t)], \quad (10)$$

and $\alpha = x, y,$ and z . $\phi[r_{ij}(t)]$ is the potential energy between particles i and j at time t . Then the new thermal conductivity is given by

$$\lambda = \frac{V}{kT^2} \int_0^\infty dt \sum_i \langle \dot{q}_{i\alpha}(0) \cdot \dot{q}_{i\alpha}(t) \rangle. \quad (11)$$

The heat flux by each molecule, Eq. (9), with the energy of molecule, Eq. (10), consists of three contributions:

$$\dot{q}_{i\alpha} = \dot{q}_{i\alpha}^{im} + \dot{q}_{i\alpha}^{pm} + \dot{q}_{i\alpha}^{ii} \quad (12)$$

where

$$\dot{q}_{i\alpha}^{im} = \frac{1}{V} \left[\frac{p_i^2}{2m_i} \right] v_{i\alpha}, \quad (13)$$

$$\dot{q}_{i\alpha}^{pm} = \frac{1}{V} \left[\frac{1}{2} \sum_{j \neq i} \phi(r_{ij}) \right] v_{i\alpha}, \quad (14)$$

and

$$\dot{q}_{i\alpha}^{ii} = \frac{1}{V} \left[\frac{1}{2} \sum_{j \neq i} r_{ij\alpha} (v_i \cdot f_{ij}) \right], \quad (15)$$

$\dot{q}_{i\alpha}^{im}$ and $\dot{q}_{i\alpha}^{pm}$ are the translational and the potential energy transport due to molecular motion, respectively, and $\dot{q}_{i\alpha}^{ii}$ is the translational energy transfer due to molecular interaction. Hence, the thermal conductivity, Eq. (11), consists of three contributions:

$$\lambda_{tot} = \lambda_{im} + \lambda_{pm} + \lambda_{ii}. \quad (16)$$

Molecular Models and Molecular Dynamics Simulation

We have considered 5 members of the noble gas family – He, Ne, Ar, Kr, and Xe – to carry out MD simulations at $T = 273.15$ and $p = 1.00$ atm. The usual Lennard-Jones (LJ) 12-6 potential for the interaction between noble gases is used with the LJ parameters,¹⁴ σ (nm) and ε/k_B (K), shown in Table 1, where k_B is the Boltzmann constant. The inter-atomic

Table 1. Lennard-Jones parameters, system constants at 273.15 K and 1 atm, and L obtained from NpT MD simulations at 1.00 atm and p obtained from NVT MD simulations using the obtained L from NpT MD. The last two columns present the Lennard-Jones potential and the total energies of each system. ρ_m and M are density and molecular mass, respectively

Gases	LJ parameters		ρ_m (kg/m ³)	M/ρ_m (l/mol)	L (nm)	L (nm), NpT	p (atm), NVT	- E_{LJ} (kJ/mol)	E_{total} (kJ/mol)
	σ (nm)	ε/k_B (K)							
He	0.2551	10.2	0.1785	22.423	40.071	40.066	1.0004	0.0000	3.406
Ne	0.2820	32.8	0.8999	22.424	40.072	40.064	1.0004	0.0007	3.406
Ar	0.3405	119.8	1.7837	22.396	40.055	40.064	0.9992	0.0058	3.401
Kr	0.3655	178.9	3.74	22.406	40.061	40.064	0.9960	0.0147	3.392
Xe	0.4047	231.0	5.86	22.405	40.060	40.064	0.9920	0.0288	3.378

potential is truncated at 1.0 nm, which is the cut-off distance used in many other simulations. Long-range corrections are applied to the energy, pressure, etc. due to the potential truncation.¹⁵ The preliminary canonical ensemble (NVT fixed) MD simulations of 1728 noble gases using a leap-frog algorithm¹⁶ were started for equilibration in the cubic box of length $L = 40.066$ nm, of which the densities are given in Table 1 at 273.15 K and 1 atm.

The equations of motion were solved using a fifth-order predictor-corrector Gear integration¹⁷ for NpT MD simulations at 1.00 atm to determine the volumes of the systems with a time step of 10^{-14} second (0.5×10^{-14} second for Ne and 0.25×10^{-14} second for He). Then it was switched to a velocity Verlet algorithm¹⁸ for NVT MD simulations with the determined volumes. The configurations of the noble gases were stored every 10 time steps (every 20 time steps for Ne and every 40 time steps for He) for further analysis. The systems were fully equilibrated and the equilibrium properties are averaged over five blocks of 400,000 time steps (800,000 for Ne and 1,600,000 for He).

Results and Discussion

The molar volumes (M/ρ_m) of noble gases and lengths of simulation box (L) calculated from ρ_m (density) and M (molecular mass) are listed in Table 1 and the values of M/ρ_m are slightly deviated from Avogadro's hypothesis (22.414 l/mol). The brief results of L (nm) obtained from NpT MD simulations at 1.00 atm and p (atm) obtained from NVT MD simulations using the obtained L from NpT MD at $T = 273.15$ are also given in Table 1. The values of (M/ρ_m) calculated from the obtained L (40.066 and 40.064 nm) from NpT MD are 22.414 and 22.411 l/mol which are almost the same as Avogadro's hypothesis (22.414 l/mol). Also, a brief summary for energetic averages is given in the last two columns of Table 1. The Lennard-Jones (LJ) potential of each system is negligibly small compared to the total energy,

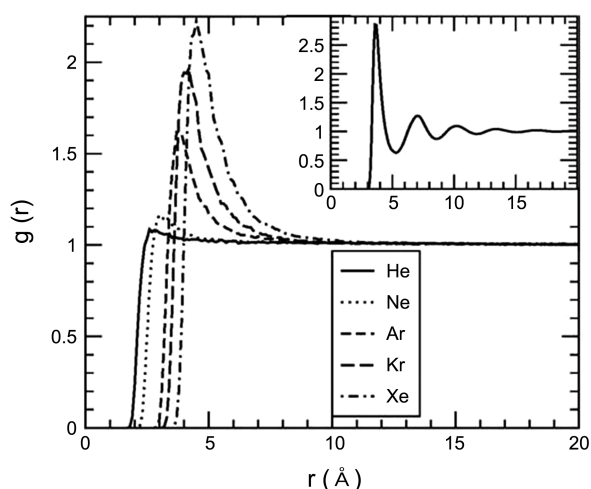


Figure 1. Radial distribution functions (RDF) of noble gases at 273.15 K and 1.00 atm. The inset shows RDF of liquid argon at 94.4 K and 1.374 g/cm³.⁴

which reflects that the most portion of the total energy is the kinetic energy. Note the kinetic energy calculated from $3RT/2$ is 3.407 kJ/mol at 273.15 K. As the size of the noble gas increases, the LJ potential energy increases slowly.

Figure 1 shows the radial distribution functions (RDF) of noble gases at 273.15 K and 1 atm. While the first peaks of He and Ne are negligibly small, those of Ar, Kr, and Xe increase with increasing size of the noble gas, but there is no second peak for all the noble gases. This indicates that there is no packing effect in gaseous state which is a typical behavior of liquid state as shown in the inset of Figure 1 for the RDF of liquid argon at 94.4 K and 1.374 g/cm³ (Fig. 2 in Ref. 4).

The rigorous results of the kinetic theory from molecular collision for transport properties of gases¹⁹ are given by

$$D = \frac{3}{8} \left(\frac{k_B T}{\pi m} \right)^{1/2} \frac{1}{\sigma^2 \rho}, \quad (17)$$

$$\eta = \frac{5}{16} \left(\frac{m k_B T}{\pi} \right)^{1/2} \frac{1}{\sigma^2}, \quad (18)$$

and

$$\lambda = \frac{25}{32} \left(\frac{k_B T}{\pi m} \right)^{1/2} \frac{C_v}{N_o \sigma^2}, \quad (19)$$

where ρ is the number density, C_v is the molar heat capacity (12.47 J/K·mol), and N_o is the Avogadro's number.

Mean square displacements (MSD) and velocity auto-correlation (VAC) of the noble gases at 273.15 K and 1 atm are plotted in Figures 2 and 3. The behaviors of MSD and VAC are remarkably different from those of liquid argon at 94.4 K and 1.374 g/cm³ (Figs. 3 and 4 in Ref. 4) as shown in the insets of Figures 2 and 3. While the mean square displacement (MSD) of liquid argon shows a linear behavior within 3 ps (see the inset of Fig. 2 or Fig. 3 in Ref. 4), the MSD of gaseous argon increases nonlinearly over 500 ps and shows a straight line between 1000 and 3000 ps. The velocity auto-correlation (VAC) function also shows a

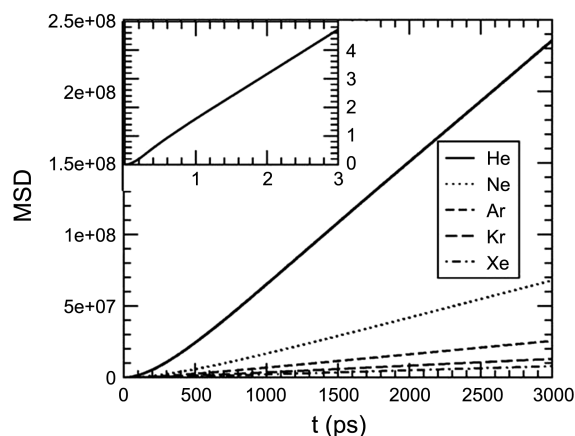


Figure 2. Mean square displacements (MSD, Å²) of noble gases at 273.15 K and 1.00 atm. The inset shows MSD of liquid argon at 94.4 K and 1.374 g/cm³.⁴

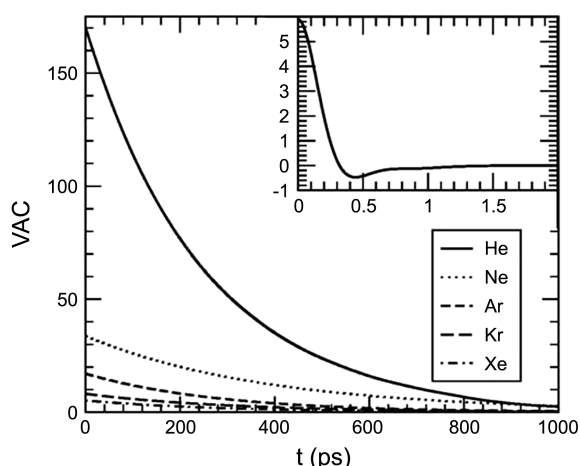


Figure 3. Velocity auto-correlation (VAC, $(10 \text{ \AA/ps})^2$) functions of noble gases at 273.15 K and 1.00 atm. The inset shows VAC of liquid argon at 94.4 K and 1.374 g/cm^3 .⁴

dramatic difference. The VAC of liquid argon decays to 0 within 0.5 ps and has a negative value due to the collision with the neighboring particle (see the inset of Fig. 3 or Fig. 4 in Ref. 4), but the VAC of gaseous argon decays very slowly to 0 over 1000 ps.

Diffusion coefficients of the noble gases at 273.15 and 293.15 K obtained from MSD's using Eq. (3) and VAC's using Eq. (4) are in good agreement with the experimental measures¹⁹ and are superior to the predictions of the kinetic theory from molecular collision, Eq. (17), as compared in Tables 2 and 3. The temperature dependence of D obtained from our MD simulations is in the range of 1.11-1.18 which is much larger than that predicted by the kinetic theory [$(293.15/273.15)^{1/2} \sim 1.04$ in Eq. (17)], even though there is

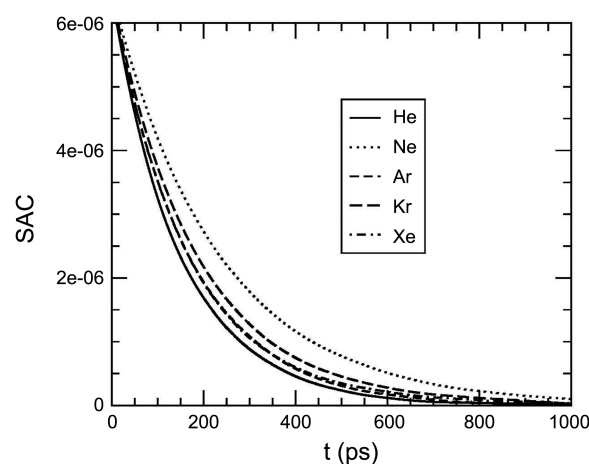


Figure 4. Stress auto-correlation (SAC, $(\text{J/mol}\cdot\text{\AA}^3)^2$) functions of noble gases at 273.15 K and 1.00 atm.

no experimental results for D at 293.15 K.

Stress auto-correlation (SAC) and heat-flux auto-correlation (HFAC) functions of the noble gases at 273.15 K and 1 atm are plotted in Figures 4 and 5. Both correlation functions are monotonically decreased and decays very slowly to 0 over 1000 ps like VAC in Figure 3. In Figure 4, the two curves of SAC for Ar and Xe at 273.15 K and 1 atm are hardly distinguishable but the latter is slightly higher over 600-1000 ps than the former, which results in the difference in the obtained viscosities of 165 (Ar) and 171 μP (Xe) in Table 2 through Eq. (8).

We plot the viscosities, η (μP), of the noble gases as a function of σ (nm) in Figure 6. The result for η obtained from our MD simulations underestimates the experimental measure²⁰ approximately 80%, but the trend of η as a

Table 2. Comparison of diffusion coefficients, viscosities, and thermal conductivities of noble gases at $T = 273.15 \text{ K}$ and 1.00 atm in NVT MD simulations with experiment and theory

Gases	D (cm^2/s)			η (μP)			λ ($\text{J/m}\cdot\text{s}\cdot\text{K}$)		
	MSD/VAC	Exp. ^a	Theory	SAC	Exp. ^b	Theory	HFAC	Exp. ^b	Theory
He	1.42(1)/1.41(5)	-	0.912	152(12)	187	136	0.1261(32)	0.1442	0.1056
Ne	0.429(7)/0.447(15)	0.452	0.332	244(6)	298	249	0.0406(13)	0.0465	0.0385
Ar	0.156(2)/0.154(8)	0.157	0.162	165(4)	210	240	0.0143(6)	0.0163	0.0188
Kr	0.0789(13)/0.0793(8)	0.080	0.097	185(4)	234	302	0.0077(2)	0.0087	0.0112
Xe	0.0479(7)/0.0468(5)	-	0.063	171(4)	212	309	0.0046(5)	0.0052	0.0073

^aRef. 19. ^bRef. 20.

Table 3. Comparison of diffusion coefficients, viscosities, and thermal conductivities of noble gases at $T = 293.15 \text{ K}$ and 1.00 atm in NVT MD simulations with experiment and theory

Gases	D (cm^2/s)			η (μP)			λ ($\text{J/m}\cdot\text{s}\cdot\text{K}$)		
	MSD/VAC	Exp.	Theory	SAC	Exp. ^b	Theory	HFAC	Exp.	Theory
He	1.61(1)/1.68(4)	-	0.945	160(8)	196	141	0.1370(98)	-	0.1094
Ne	0.476(12)/0.480(8)	-	0.344	255(5)	313	258	0.0420(12)	-	0.0399
Ar	0.180(6)/0.180(11)	-	0.168	173(11)	223	249	0.0153(10)	-	0.0194
Kr	0.0928(11)/0.0909(9)	-	0.100	194(9)	250	313	0.0081(3)	-	0.0117
Xe	0.0535(2)/0.0531(18)	-	0.065	180(11)	228	320	0.0047(2)	-	0.0076

^bRef.20.

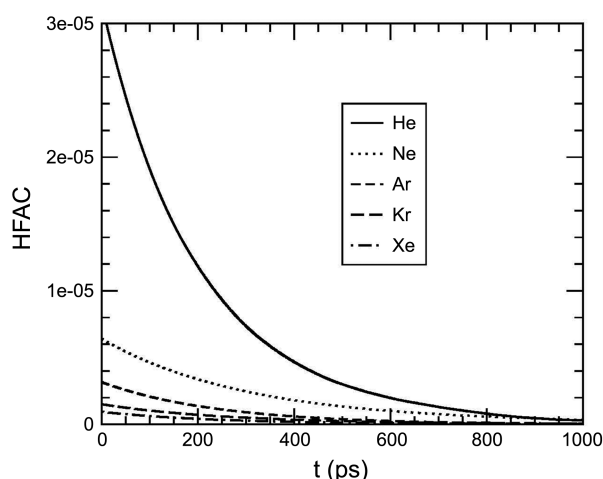


Figure 5. Heat-flux auto-correlation (HFAC, $(10 \text{ J/mol}\cdot\text{\AA}^2\cdot\text{ps}^2)$) functions of noble gases at 273.15 K and 1.00 atm.

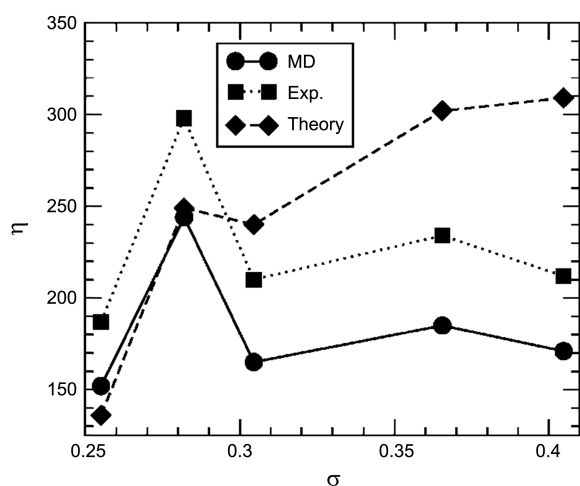


Figure 6. Viscosities (μP) of noble gases at 273.15 K and 1.00 atm as a function of σ (nm).

function of σ shows the exact agreement with that of the experimental result. The value of η for He, η_{He} , is the smallest, η_{Ne} the largest, η_{Ar} decreased, η_{Kr} increased slightly, and η_{Xe} decreased again, larger than η_{Ar} . This trend is exactly predicted from the SAC functions of the noble gases in Figure 4 by integrating the curves. However, the behavior of the SAC function as a function of σ is not fully understood in this study. It is obviously related to the pressure tensor, $P_{i\alpha\beta}$. The prediction from the kinetic theory shows a good agreement with results of MD simulations for η_{He} and η_{Ne} but overestimates the experimental²⁰ measure and the MD result for η_{Ar} , η_{Kr} , and η_{Xe} . The temperature dependence of η obtained from our MD simulations is approximately 1.05 and the dependence of experimental results for η is in the range of 1.05-1.08 but it is $[(293.15/273.15)^{1/2} \sim 1.04]$ in Eq. (18) by the kinetic theory.

Unlike the SAC functions, the HFAC functions are easily distinguishable like the VAC and the result for λ obtained from our MD simulations underestimates the experimental measure²⁰ approximately 88%. As predicted from the behavior

of the ideal gas, the contributions to the thermal conductivity from the potential energy transport due to molecular motion (λ_{pm}) and from the translational energy transfer due to molecular interaction (λ_{ti}) are essentially zero because of the null of molecular interaction. Hence, only the contribution from the translational energy transport due to molecular motion exists, $\lambda_{tot} = \lambda_{tm}$. The prediction from the kinetic theory underestimates the experimental measure²⁰ and the MD result for λ_{He} and λ_{Ne} , but overestimates those results for λ_{Ar} , λ_{Kr} , and λ_{Xe} .

Conclusion

We have carried out a series of equilibrium molecular dynamics (EMD) simulations of noble gases (He, Ne, Ar, Kr, and Xe) at 273.15 K and 1.00 atm for the calculation of transport properties. The structural and dynamic properties of noble gases are completely different from those of liquid argon at 94.4 K and 1.374 g/cm³. While the diffusion coefficients (D) of noble gases was obtained through the original Green-Kubo formula, the viscosities (η) and thermal conductivities (λ) were obtained by utilizing the revised Green-Kubo formulas. The results for transport properties (D , η , and λ) at 273.15 and 1.00 atm obtained from our EMD simulations are in general agreement with the experimental data and superior to the rigorous results of the kinetic theory. The trend of η as a function of σ obtained from simulations shows the exact agreement with that of the experimental result. The contributions to the thermal conductivity from the potential energy transport due to molecular motion (λ_{pm}) and from the translational energy transfer due to molecular interaction (λ_{ti}) are essentially zero because of the null of molecular interaction.

Acknowledgments. This research was supported by Kyungshung University Research Grants in 2013.

References

- Allen, M. P.; Tildesley, D. J. *Computer Simulation of Liquids*; Oxford Univ. Press: Oxford, 1987; p 2.
- Alder, B. J.; Wainwright, T. E. *J. Chem. Phys.* **1957**, *27*, 1208.
- Alder, B. J.; Wainwright, T. E. *J. Chem. Phys.* **1959**, *31*, 459.
- Rahman, A. *Phys. Rev. A* **1964**, *136*, 405.
- Verlet, L. *Phys. Rev.* **1967**, *159*, 98.
- Verlet, L. *Phys. Rev.* **1968**, *165*, 201.
- Nicolas, J. J.; Gubbins, K. E.; Streett, W. B.; Tildesley, D. J. *Mol. Phys.* **1979**, *37*, 1429.
- Harp, G. D.; Berne, B. J. *J. Chem. Phys.* **1968**, *49*, 1249.
- Berne, B. J.; Harp, G. D. *Adv. Chem. Phys.* **1970**, *17*, 63.
- Barker, J. A.; Watts, R. O. *Chem. Phys. Lett.* **1969**, *3*, 144.
- Rahman, A.; Stillinger, F. H. *J. Chem. Phys.* **1971**, *55*, 3336.
- Lee, S. H.; Park, D. K.; Kang, D. B. *Bull. Korean Chem. Soc.* **2003**, *24*, 178.
- Lee, S. H. *Bull. Korean Chem. Soc.* **2007**, *28*, 1371.
- Hirschfelder, J. O.; Curtiss, C. F.; Birds, R. B. *Molecular Theory of Gases and Liquids*; John Wiley: NY, 1954; pp 1110 & 1212.
- Allen, M. P.; Tildesley, D. J. *Computer Simulation of Liquids*; Oxford Univ. Press: Oxford, 1987; p 64.
- Allen, M. P.; Tildesley, D. J. *Computer Simulation of Liquids*;

- Oxford Univ. Press: Oxford, 1987; p 80.
17. Gear, C. W. *Numerical Initial Value Problems in Ordinary Differential Equation*; Prentice-Hall: Englewood Cliffs, NJ, 1971.
 18. Allen, M. P.; Tildesley, D. J. *Computer Simulation of Liquids*; Oxford Univ. Press: Oxford, 1987; p 81.
 19. McQuarrie, D. A. *Statistical Mechanics*, 2nd ed; Happer & Row: NY, 1976; pp 364-365.
 20. Atkins, P. W.; de Paula, J. *Physical Chemistry; Vol. 1 Thermodynamics and Kinetics*, 8th ed; Oxford Univ Press: Oxford, 2006; p 452.
-